Icosahedral $(H_2)_{13}$ supermolecule

HPSTAR 632-2018

Graeme J. Ackland,[1] Jack Binns,[2] Ross Howie,[2] and Miguel Martinez-Canales[1]
[1]*CSEC, School of Physics and Astronomy, The University of Edinburgh, Edinburgh EH9 3FD, United Kingdom*
[2]*Center for High Pressure Science Technology Advanced Research (HPSTAR), Shanghai, China*

(Received 17 March 2018; revised manuscript received 3 July 2018; published 4 September 2018)

We investigate a range of possible materials containing the supermolecular form of hydrogen comprising 13 H_2 molecules arranged in an icosahedral arrangement. This supermolecule consists of freely rotating 12 H_2 molecules in an icosahedral arrangement, enclosing another freely rotating H_2 molecule. To date, this supermolecule has only been observed in a compound with iodane (HI). The extremely high hydrogen content suggests possible application in hydrogen storage so we examine the possibility of supermolecule formation at ambient pressures. We show that *ab initio* molecular dynamics calculations give a good description of the known properties of the $HI(H_2)_{13}$ material, and we make predictions of the existence of the related compounds $Xe(H_2)_{13}$, $HBr(H_2)_{13}$, and $HCl(H_2)_{13}$, including a symmetry-breaking phase transition at low temperature. The icosahedral $(H_2)_{13}$ supermolecule remains stable in all these compounds. This suggests $(H_2)_{13}$ is a widespread feature in hydrogen compounds and that appropriately sized cavities could hold hydrogen supermolecules even at low pressure. The structure of the supermolecule network is shown to be independent of the compound at equivalent density.

DOI: 10.1103/PhysRevMaterials.2.093601

I. INTRODUCTION

Hydrogen-rich compounds have attracted a lot of attention because of their potential applications for fuel cell storage [1] and for high-T_c superconductors [2]. In particular, high pressure has been an effective thermodynamic variable in the synthesis of such compounds exemplified by recent experimental and theoretical breakthroughs [1–15].

The developments in high-pressure diamond anvil cells have pushed the frontiers, with pressures up to 200 GPa now obtained routinely for most materials. However experimental studies involving hydrogen prove both problematic and costly, through the premature failure of the anvils due to hydrogen diffusion and embrittlement. Computational structure searches based on density functional theory have now assumed an important role as a screening method in finding materials of potential interest as targets for synthesis [16,17] and first suggested very large hydrogen fraction compounds as a route to high-T_c superconductivity or energy storage [18].

Recently, Binns *et al.* [14] synthesized $HIH(_2)_{13}$, a compound with a number of remarkable features. At over 96% stoichiometric ratio, it has the highest known molecular hydrogen content of any compound. While this stoichiometry suggests IH_{27} to be a solid solution, x-ray diffraction shows a primitive cubic lattice of iodine atoms [14]. The material can be regarded as a 1:1 stoichiometric compound comprising iodane molecules and so-called $(H_2)_{13}$ supermolecules. Assuming that each H_2 is spherical, as is the case for phase I of solid hydrogen, three obvious possibilities present themselves for the supermolecule: cuboctahedron, icosahedron, or dynamically spherical. Icosahedral symmetry would be curious, because the fivefold symmetry is incompatible with the cubic structure. The structure suggested by simulation has a doubled unit cell along {111}, with two icosahedral supermolecules in opposite orientations: this more complex structure is fully compatible with existing experimental x-ray (which cannot detect the hydrogen positions) and Raman experimental data.

Hydrogen-storage materials face an intrinsic trade-off between strongly binding hydrogen (atomic or molecular) for stability and the energy required to release H_2 for applications. The $(H_2)_{13}$ units are especially attractive because they store a large amount of hydrogen in a weakly bound molecular form. Other hydrogen-rich materials such as methane hydrates or ammonium borohydride require energy to break strong bonds between the hydrogen and other elements [1,19].

It is interesting to consider whether the supermolecules may be recovered to ambient conditions in any material. $HI(H_2)_{13}$ decomposes on depressurization, but this may be because the HI molecule itself is unstable to decomposition to H_2 and I_2 at ambient conditions [20]. Since the nature of the binding in this material remains unknown, it is unclear whether this lack of recoverability is a necessary consequence of the bonding type or if other similar materials might be recoverable. Replacing the iodane molecule with something stable is an obvious first step, e.g., other hydrogen halides, large metallic atoms, noble gases, or small polar molecules like chloromethane.

Here, we show that density functional theory (DFT) and *ab initio* molecular dynamics (AIMD) produce an accurate description of the known $HI(H_2)_{13}$ compound and analysis of its behavior under depressurization. Using these results, we investigate other potential compounds that could exhibit this hydrogen supermolecule and find $HBr(H_2)_{13}$, $HCl(H_2)_{13}$, and $Xe(H_2)_{13}$ to all be dynamically stable. The unprecedented stability of these compounds suggests that $(H_2)_{13}$ may be exhibited in a variety of systems and, if recoverable, could have potential uses in hydrogen storage applications.

 ©2018 American Physical Society

II. METHODS

DFT calculations were performed using the CASTEP plane-wave pseudopotential package [21], using norm-conserving pseudopotentials, a minimum of $2\times2\times2$ k-points, and an energy cutoff of 1200 eV. Temperature and anharmonic effects were accounted for by performing Born-Oppenheimer AIMD, using a 0.5-fs time step. AIMD runs were typically 3 ps long. This is necessarily far too short of experimental timescales, but is much longer than any characteristic oscillation in the system, such that any soft-phonon or martensitic transition could easily occur. It is also long enough to observe the free rotation of H_2 molecules. We used a $2\times2\times2$ supercell with eight supermolecular units (224 atoms).

In all cases, the heavy molecules form a time-averaged structure close to simple cubic, so for ease of comparison throughout, we always report the lattice parameter associated with this lattice. This is also the only structural variable that can be determined from x-ray diffraction because the H_2 molecules are essentially invisible to x rays.

The choice of exchange correlation functional is a highly debated topic in DFT studies of hydrogen. In a benchmarking study on hydrogen the Becke–Lee-Yang-Parr (BLYP) functional [22,23] was shown to give results closest to quantum Monte Carlo calculations [24,25], for transition pressures and vibrational frequencies, due mainly to the correct asymptotic behavior at high charge density gradient [26].

Van der Waals interactions are not well accounted for in traditional semilocal exchange-correlation functionals. These, however, could be important in holding the hydrogen molecules together. It has been shown that explicit nonlocal treatment of the van der Waals interaction is of secondary importance for hydrogen at pressures beyond 200 GPa [26]. The calculations shown here are performed with the BLYP functional unless otherwise stated, with other exchange-correlation functionals [27–30] used for comparison in some configurations (Fig. 1). As expected, we find Tkatchenko-Scheffler van der Waals corrections produce no significant differences over the other semilocal functionals. The radial distribution function (RDF) shown in Fig. 1 shows that, at a given volume, the structural details are effectively independent of the functional. There is a bigger discrepancy in the computed DFT pressure. The BLYP functional gives by far the largest values and consequently a much higher "pressure" at a given density compared with other functionals or with experimental data. Pressure is a derived quantity in DFT, whereas volume is directly input, so it is reasonable to compare calculations at the same density.

In AIMD at 300 K, we observe that the hydrogen forms well-defined molecules with a high-frequency, Raman-active stretching mode (vibron). Molecules behave as mildly inhibited rotors, so we expect their Raman signature to be that of a quantum rotor (roton) at low pressure and that of a rotating harmonic oscillator (libron) at higher pressures. This also means that the molecules exhibit the correct spherical symmetry and that, over time, the indistinguishability of the two nuclei is respected. It is not clear to what extent the single-molecule angular momentum J is a good quantum number, but in any case fully quantum treatment with ortho- and para-hydrogen is not currently possible. Below 100 K, molecular rotation stops, and orientations are frozen into a rotational glass.

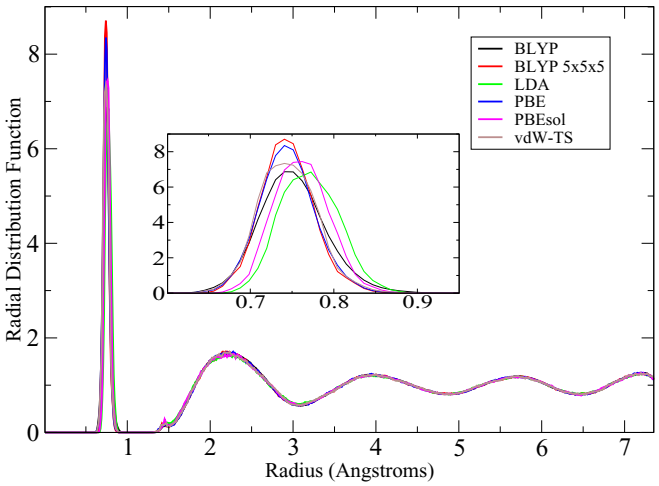

FIG. 1. All-atom RDF in $HBr(H_2)_{13}$ at lattice parameter 5.25 Å, calculated with a variety of exchange-correlation functionals. The small feature at 1.5 Å is the HBr bond. The calculated pressures are 16.7 GPa (BLYP, [22,23], 5^3 k-point grid), 20.5 GPa (BLYP [22,23]), 16.4 GPa (PBE, Perdew-Burke-Ernzerhof [27]), 11.3 GPa (LDA, local-density approximation [29]), 13.3 GPa (PBEsol, Perdew-Burke-Ernzerhof refitted to a database of solids [28]), and 15.3 GPa (PBE + TS, Tkatchenko-Scheffler van der Waals corrections [30]). Inset: Detail for the first peak, showing that LDA and PBEsol give noticeably longer bond lengths commensurate with their lower pressures. Molecular dynamics simulations are fixed number, volume, temperature ensemble (NVT) at 300 K, equilibrated for 1 ps, and then averaged over 1.5 ps, and they contain eight supermolecules.

Quantum nuclear effects are neglected in classical molecular dynamics (MD), and there are several distinct places to consider where this can be problematic [31].

(i) The high-frequency H_2 molecular vibration is thermally excited in classical MD, but essentially not in the quantum case. It adds a spurious contribution to the heat capacity, which is therefore not reliable, and a zero-point energy contribution to the total energy. However, these contributions are essentially the same in all structures and so cancel out in the free-energy differences which determine stability.

(ii) The volume dependence of the zero-point motion makes a contribution to the pressure. This is significant at pressures above 200 GPa where the H_2 vibron weakens significantly [31]. At lower pressures, it is of order 1 GPa, close to the uncertainty due to the exchange-correlation functional.

(iii) The zero-point motion means that there is already some energy in the bond, so breaking it would be easier if quantum nuclear effects were considered. However, in our simulations we do not see significant bond breaking.

(iv) Noninteracting hydrogen molecules behave as quantum rotors with energy $\hbar^2 J(J+1)/2I$, where I is the moment of inertia. The first excited state has energy around 170 K (H_2) or 85 K (other molecules), so the thermal excitation implied by our 300 K classical simulations are reasonable. Furthermore, the classical free rotor behavior is a good representation of the spherically symmetric $J=0$ ground state. Thus we expect our supermolecule calculations to correctly describe the symmetry, just as classical MD of solid hydrogen gave an accurate qualitative prediction for the melting point of

the "quantum rotor" phase [32]. By contrast, cooling simulations which show a symmetry-breaking phase transition are likely to overestimate the transition temperature.

(v) The requirement for antisymmetic wave functions means that the nuclear spin states of ortho- and para-hydrogen couple to even and odd J states, respectively. This causes a slow equilibration of the roton energy. However, it only applies when J is a good quantum number. We monitor the angular momentum autocorrelation and find that typically the classical rotor cannot complete a full rotation without decorrelating. Thus the rotors are coupled, J is not a good quantum number, only the wave function of the entire system need be antisymmetric, and the nuclear spin state does not affect the dynamics.

So we expect any predictions of room-temperature structures to be robust with regard to quantum nuclear effects.

The DFT calculations give reliable indications of stability, but to obtain further insight one must look beyond the standard outputs to consider the nature of the bonding. Pure high-pressure hydrogen changes under pressure from normal molecular phases to phases in which the electron is squeezed out of the bond, making it weaker and longer [6,7,33–38].

We have developed some techniques for imaging and analyzing rotating molecules. All of these depend on being able to identify H_2 molecules. To do this, we first identify the nearest neighbor of each iodine. Then, we find the nearest neighbor of each remaining hydrogen atom. Provided each atom is its neighbor's neighbor, this uniquely defines molecules. This procedure works at all but a few time steps at the highest pressures and temperatures considered here, when H-H bond reconstruction sometimes occurs. Such transforming configurations are excluded from the statistics.

Once molecules are identified, we can define the length r_k and the angular momentum $\mathbf{l}_k$ for each molecule k. For the vibrons, we exploit the fact that Raman activity involves an in-phase symmetric stretch of all the molecules. We sum the total length of all molecules and build the velocity autocorrelation function (VACF),

$$\mathrm{VACF}(t) = \left\langle \frac{d}{dt}\sum_k r_k(t) - \frac{d}{dt}\sum_k r_k(0) \right\rangle,$$

and the autocorrelation of the angular momentum (LACF),

$$\mathrm{LACF}(t) = \left\langle \frac{d}{dt}\sum_k \mathbf{l}_k(t) - \frac{d}{dt}\sum_k \mathbf{l}_k(0) \right\rangle.$$

The peaks in the Fourier transform of the VACF correspond to the Raman-active vibron modes [35], where $\mathbf{l}_k$ is the angular momentum of molecule k with respect to its center of mass. Interpretation of the LACF is more subtle. If we had nonrotating molecules, its Fourier transform would give the librational mode frequencies. For free rotors the quantized energies are unrelated to the period of rotation and are simply $J(J+1)\hbar^2/mr_k^2$. In the rotor case, the LACF tells us for how long the molecule rotates unhindered.

A. The known material $HI(H_2)_{13}$

The only currently known material containing the $(H_2)_{13}$ supermolecule is $HI(H_2)_{13}$. The material was synthesized by chemical reaction at pressure inside a diamond anvil cell [14].

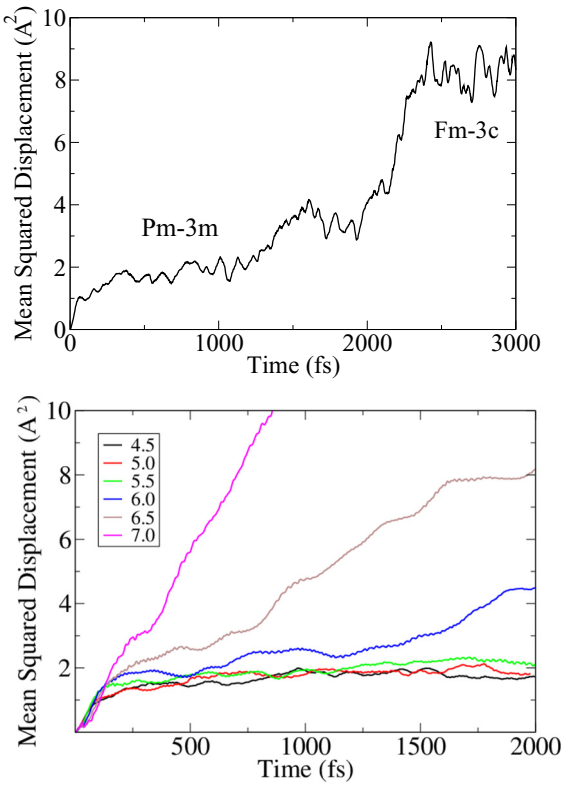

FIG. 2. (a) MSD discontinuity at 2200 fs showing transformation of the supermolecule in $HI(H_2)_{13}$ from cuboctahedral to icosahedral. (b) MSD for $HCl(H_2)_{13}$ at 300 K and a range of lattice parameters, in Å, as shown in the legend. The divergent MSDs correspond to low pressures below 7 GPa.

The simple-cubic arrangement of the iodine atoms was observed by x-ray diffraction, and the iodane and hydrogen molecules were identified by their characteristic Raman vibron frequencies. The composition was determined by matching the density to the known I_2 and H_2 equations of state. The atomic arrangement was deduced from MD simulations, which support free IH and H_2 rotors at 300 K. Binns *et al.* [14] demonstrated the *average* icosahedral symmetry of the supermolecule by plotting the mean *atomic* positions: for a free-rotating HI molecule, the mean H position is close to the center of the iodine, while for H_2 the mean position of both atoms is the same: the molecular center.

In analogy with other binary AB_{13} systems [39–43] two clear candidate structures involving cuboctahedral ($Pm\bar{3}m$) and icosahedral ($Fm\bar{3}c$) $(H_2)_{13}$ supermolecules emerge. In order to find out the favored structure, we carried out NPT *ab initio* molecular dynamics simulation on these two phases at 30 GPa and 300 K, using the Perdew-Burke-Ernzerhof (PBE) functional. Using a primitive cubic cell, both $Pm\bar{3}m$ (28 atoms) and $Fm\bar{3}c$ (56 atoms) remained stable over 3 ps. Using a larger cell with 224 atoms compatible with either structure, simulations started with cuboctahedral supermolecules spontaneously transformed to icosahedral ones. The molecular rearrangement is abrupt and can be seen in the mean square displacement (MSD) shown in Fig. 2. This proves that the $Fm\bar{3}c$ structure, with two oppositely aligned icosahedral supermolecules, is the stable structure.

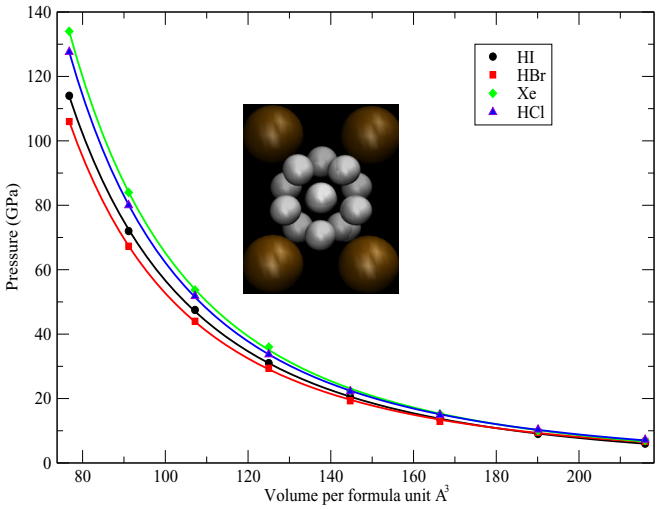

FIG. 3. Equations of state calculated using the BLYP functional. The relative ordering of the curves is independent of the functional, but other functionals tested give lower values of pressure, so the systematic error in the calculated pressure is of the order of ±5 GPa. Symbols are calculated pressure averages with the statistical error less than the symbol size. Lines show fits to the Murnaghan equation of state. The inset shows the mean atomic positions for $IH(H_2)_{13}$, emphasizing the fivefold axis of the supermolecule.

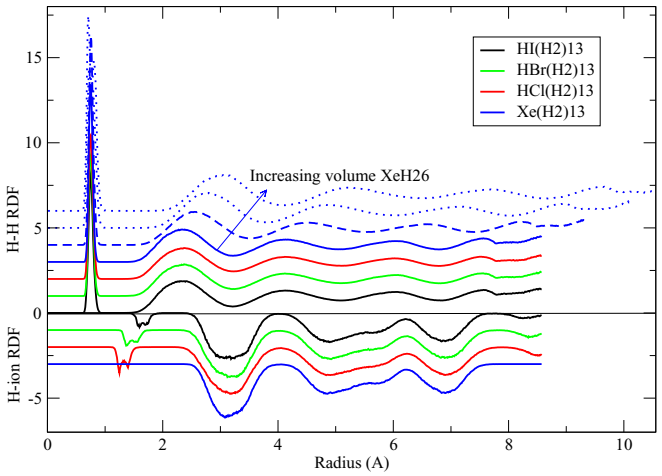

FIG. 4. Radial distribution functions for hydrogen H-H (top panel) and H-X (bottom panel, X = Cl, I, Br, Xe) for different compounds at the same lattice parameter (5.5 Å) and for the same compound, $Xe(H_2)_{13}$, at different densities (top lines in the upper panel).

We then examined the possibility of recovering of the supermolecule. This was done using a series of calculations at 300 K in the NVT ensemble, using the BLYP functional, and gradually reducing the density. [Results are similar to the $HCl(H_2)_{13}$ data in Fig. 2(b); movies are available in the Supplemental Material [44]). At lattice parameters greater than 7 Å, the structure becomes unstable.

We found that $HI(H_2)_{13}$ remains stable in a pressure range between 6 and 100 GPa. The equation of state is shown in Fig. 3. We used the projection method to calculate the vibrational frequencies of the Raman-active vibrons. This showed that the two hydrogen environments have very similar vibrational frequencies, and we were unable to distinguish a doublet. The frequency is significantly different from pure hydrogen at the same pressures. The HI vibron provides a well-defined signature for iodane. We also did one run setting the iodine mass to that of hydrogen: although the dynamics are affected, in classical Born-Oppenheimer MD, the free-energy landscape is mass independent, so this is equivalent to sampling for 200 ps—still no structural transformation occurred.

B. Predicted compounds: $HBr(H_2)_{13}$, $HCl(H_2)_{13}$, and $Xe(H_2)_{13}$

Having established that molecular dynamics can determine the stability of the supermolecule phases, we investigated a number of other possible materials based on the same structure. The dynamic nature of the structure means that standard methods of *ab initio* structure searching for static lattices cannot describe the symmetry. So we resorted again to molecular dynamics to determine the metastability of the structures.

At higher pressures, all three tested compounds were found to remain stable throughout the simulations (up to 6 ps) at high pressures, but at lower pressures the molecules began to exchange positions within and between icosahedra, effectively forming a solution of HI, HBr, or HCl in fluid hydrogen. We believe that the implication is that on longer timescales the compound will be unstable at low density. This is shown by the divergent MSD of the hydrogen atoms in $HCl(H_2)_{13}$ for lattice parameters above 6.0 Å [Fig. 2(b)]. Similar behavior is seen for both BLYP and PBE functionals at the same density. $HCl(H_2)_{13}$ is the most unstable of the materials here: equivalent calculations for $HI(H_2)_{13}$, $HBr(H_2)_{13}$, $HI(H_2)_{13}$, and $Xe(H_2)_{13}$ respectively showed the breakdown in stability occurs at increasing volume. The Xe compound did not break down, even at ambient pressure, and appears to be the most stable.

Comparative equations of state calculated with the BLYP functional are shown in Fig. 3. The three halide compounds show a clear trend in the lattice parameter, with Xe falling between the HI and HBr compounds. This scaling with molecular size is expected; much more interesting is the comparison of the RDFs.

Comparing different compounds at the same *volume* (Fig. 4), the RDFs of the structures are essentially identical, apart from the halide bond length. However, because of the different equations of state, for different compounds at the same *pressure*, the supermolecule has very different intermolecular distances. The supermolecule behavior is primarily determined by the hydrogen density: the halide molecules provide an additional *chemical pressure* which determines the total pressure at a given hydrogen density.

The equivalence of the hydrogen structure for all compounds implies that the difference in pressure is mainly attributable to the halide/Xe sublattice. Figure 4 shows that the larger IH halide compound is associated with the higher pressures. However this "molecular volume" argument is incompatible with the fact that the HI-H_2 intermolecular distances are the same as those for HBr-H_2 and HCl-H_2. Another possibility is that the materials with the higher permanent dipole moment have stronger cohesion, due to dipole-dipole correlations, and

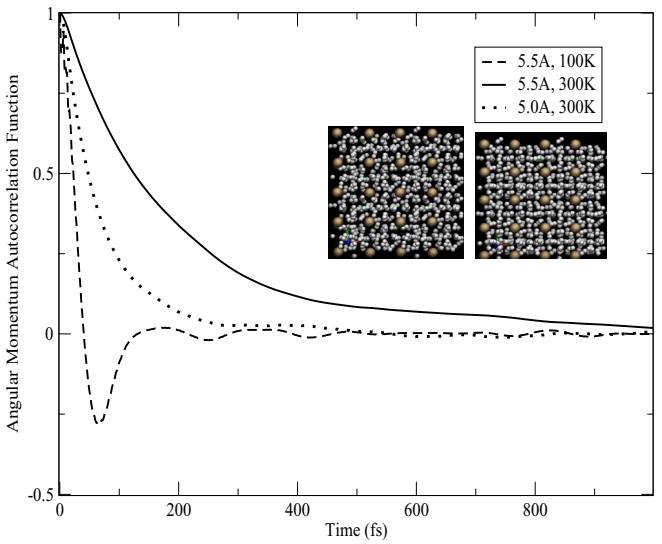

FIG. 5. LACF for $Xe(H_2)_{13}$ at 300 K (solid line) and 100 K (dashed line, inset right), with a 5.5 Å lattice parameter. The VACF at 300 K and $a = 5.0$ Å is shown for comparison. Insets are MD snapshots at 5.5 Å, showing the symmetry breaking in the hydrogen (small spheres) sublattice on cooling.

hence lower external pressure. This explanation works well for the halides, but is problematic with respect to the Xe compound which has no dipole interactions. Whatever the explanation, it is clear that the pressure at which the supermolecule is stabilized depends strongly on the other species.

III. LOW-TEMPERATURE PHASE TRANSFORMATIONS

Most free-rotor phases undergo a symmetry-breaking phase transformation when intermolecular forces are strong enough to stop the rotation. In our simulations we observed that during cooling to 100 K there is a transformation in the supermolecule to a low-temperature structure where the rotation is frozen and the molecules librate rather than rotate. This can be seen in animation (see Supplemental Material [44]) and in the angular momentum correlation functions: Fig. 5 show the results for $Xe(H_2)_{13}$ which is the most symmetric structure on account of the monatomic Xe.

In the high-T symmetric phase the molecular orientation is disordered and the rotation remains autocorrelated for a picosecond. At lower-T, the libration is shown by the negative region of the ACF and subsequent oscillation. The short correlation time indicates that the single-molecule libron is not an eigenmode. It is also notable that the correlation time for the 300 K rotor is much reduced by pressure: this will manifest experimentally as a broadening of the roton peak in spectroscopy. By 15 GPa (5.5 Å) the autocorrelation function has a half-life of less than 100 fs, which corresponds to less than a full rotation.

The Xe compound best illustrates the broken symmetry of the supermolecule $(H_2)_{13}$, since Xe is spherical. The inset in Fig. 5 shows a tendency for the molecules to align along the cubic (100) axes. The VACF-calculated Raman vibron spectrum shows two discernible peaks, separated by over 100 wave numbers, indicating that there are two distinct H_2 environments, which would be a clear experimental signature of the symmetry breaking on cooling. In the halogen compounds, the symmetry breaking is more complex because of the dipole moment.

There has been some previous experimental and theoretical work on xenon-hydrogen mixtures at lower hydrogen concentrations (90:10 gas mixtures). Somayazulu *et al.* [45,46] found compounds with stoichiometry, $Xe(H_2)_7$ or $Xe(H_2)_8$. From the scattering pattern, they deduced the existence of covalent Xe-Xe dimer bonds. A DFT structure search at these compositions found candidate structures consistent with the experimental data, but was unable to find any Xe-Xe bonding [47]. As mentioned in Sec. II, a ground-state structure search inevitably produces symmetry breaking from the orientation of the hydrogen molecules. Given the initial stoichiometries of these works, it is unlikely that the $Xe(H_2)_{13}$ compound could have been found.

IV. LATTICE DYNAMICS

The Raman-active hydrogen vibron can be calculated from the MD using the projection method [48,49]. Figure 6 shows the data for $HI(H_2)_{13}$. Only a single peak is evident, showing that the vibration of the central molecule in $(H_2)_{13}$ has the same frequency as the others. Moreover, this frequency is significantly dependent on the functional used. A typical production run of 3 ps allows a discrete Fourier transform to sample every 10 cm^{-1}. This is sufficient to produce a peak around 4100 cm^{-1}, but not to discern any trend with pressure, and so all pressures are shown together. Other functionals predict a somewhat lower frequency: 3920 and 3860 cm^{-1} for PBE and LDA, respectively. Thus despite the structural similarity, there is strong dependence of vibron frequency on the functional, correlated with a variation of 2–3% in H_2 bond length. Of these, the BLYP frequency is closest to the experimental value: 4210 ± 10 cm^{-1}. A similar calculation for pure hydrogen at 20 GPa produces the red curve in Fig. 6, and, despite the noise, it is clear that the hydrogen frequency is tens of wave numbers higher and probably sharper. The hypothetical compounds mirror this behavior: the vibron frequency is always lower for the compound than for pure hydrogen. We are not able to discern any trend difference between the compounds, suggesting that the supermolecular environment itself causes the shift.

For classical crystals, Raman intensity calculations using DFT lattice dynamics and perturbation theory are straightforward. However, the small-amplitude approximation breaks down in the limit of freely rotating molecules: consider, for example, a molecule pointing along the x direction, the normal mode corresponding to the stretching mode involves atomic displacements along $\pm x$. Suppose that later the molecule rotates to point along the y direction; now the atomic displacements along $\pm x$ would correspond to molecular rotation, not stretching. Thus Raman modes cannot be associated with Cartesian normal-mode eigenvectors. Rotons are not harmonic oscillators, and the quantized energy of a roton is not related to any classical frequency.

Although coupling between rotons and other Raman modes means one cannot simply apply standard lattice dynamics, it is instructive to make some attempt. So we extracted a

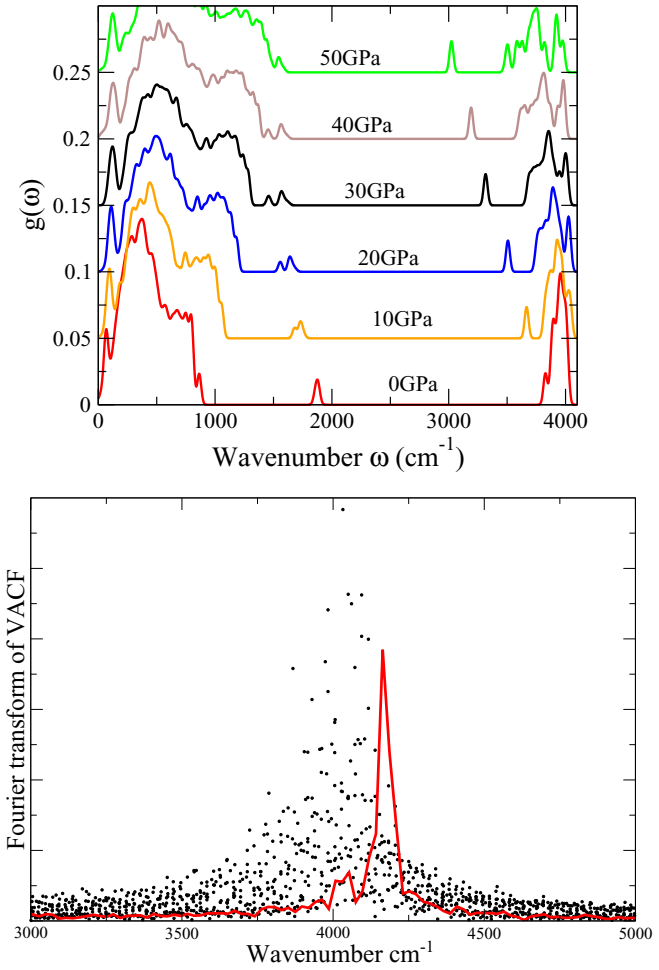

FIG. 6. (a) Phonon density of states for a snapshot from $HI(H_2)_{13}$ MD relaxed from 300 K at a range of pressures: 0, 10, 20, 30, 40, and 50 GPa. The calculation uses a PBE 3×3×3 q-point grid and Gaussian broadening with full width at half maximum of 40 cm^{-1}: since it is an MD snapshot no attempt is made to interpolate "bands." (b) Fourier transform of the VACF projected onto in-phase H_2 molecular vibrations [35], for $HI(H_2)_{13}$ (black dots) and points from discrete Fourier transforms aggregated over all pressures, and a single calculation of pure hydrogen at 20 GPa (red solid line).

snapshot from the MD calculation, relaxed it to the nearest zero-temperature enthalpy minimum for a range of pressures, and calculated the phonon density of states (DoS) between 0 and 50 GPa. The results are shown in Fig. 6. Although this is not a definitive representation of the structure, a comparison at different pressures using the same snapshot is meaningful and the phonon DoS shows a number of interesting features.

First, the main effect of pressure is to broaden the vibron band and shift it to lower frequencies. Second, the mode has a frequency much lower than that of the equivalent vibron in pure hydrogen (e.g., using identical settings the Raman mode for pure hydrogen [50] at 30 GPa is 4292 cm^{-1}). This is consistent with the observation of Binns *et al.* [14] who saw two vibrons and attributed the higher frequency mode to pure hydrogen. The H_2 molecule bond length is around 0.75 Å, compared to 0.736 Å in pure hydrogen. It suggests that the H-H bond in the supermolecule is weaker, more like that in hydrogen phase III which occurs at much greater pressure.

Our phonon calculation also shows a pronounced weakening of the IH bond with pressure, from 2000 to 1500 cm^{-1}, again consistent with experimental data. The reason for this can also be seen in by a detailed analysis of the modes. One mode in Fig. 6, corresponding to a single H_2 molecule, becomes detached from the main vibron band and significantly weakens with pressure. Interestingly, the molecule in question is *not* the one in the center of the supermolecule, rather it is the one closest to the H ion in the IH molecule. By 50 GPa, its bond length has stretched to 0.843 Å, and the Mulliken bond population is ∼25% lower than that of other molecules. Even so, this vibron has a much higher frequency than the rotation of the IH molecule. So it is reasonable to treat the IH dipole orientation as fixed throughout many vibrational periods of the vibron: in short, we believe that this bond weakening is real. The weakened H_2 bond would be difficult to detect by spectroscopy, because with a lifetime equivalent to the rotation rate of the IH, it will have a linewidth of hundreds of wave numbers, not the arbitrarily chosen 40 cm^{-1} of Fig. 6. However, as they rotate, all the IH will *always* have a nearby hydrogen, so the weakening of its bond is permanent and detectable.

Comparing the two phonon methods, we see that the projection method gives a smaller range of vibron frequencies than the lattice dynamics, as expected since they are only the Raman active modes. Using the full VACF without projection gives a broader band and the low-frequency modes, similar to the lattice dynamics. VACF also picks out the IH vibron, but not the weakening H_2 mode: this strongly suggests that the latter mode is an artifact of the snapshot used in the lattice dynamics.

V. DISCUSSION

We have shown that the icosahedral $(H_2)_{13}$ supermolecule is a unit from which to build hydrogen-rich crystal structures. The structure is similar to some AB_{13} compounds, such as $NaZn_{13}$ and beryllium-rich intermetallics. But whereas those are held together by metallic bonding, $(H_2)_{13}$ is unique in having only van der Waals or quadrupole interactions to stabilize it. An alternative reason for the stability of AB_{13} is observed in binary hard sphere mixtures and opals (packed SiO_2 spheres) because it has low entropy thanks to its dense packing [41,43].

The icosahedral, 13-member supermolecule has been calculated to be the most stable molecular cluster due to van der Waals interaction in Lennard-Jonesium and in hydrogen [51–53]. The motif cannot be extended to fill homogeneous three-dimensional space, but the current study demonstrates that, by packing alongside other molecules, extended structures can be built from this stable cluster.

In DFT calculations, the fundamental quantity is the volume. Pressure is a derived quantity, and the work emphasizes the dependence of the pressure on the exchange-correlation functional. In particular, the BLYP functional, known to give the closest agreement with the quantum Monte Carlo calculations [24,25] for dense hydrogen, gives calculated pressures higher than those of other functionals or experiments. The robust conclusions of this paper are therefore framed in terms of density rather than pressure.

The key question for understanding the prospects for recoverability is whether the supermolecule is primarily stabilized by

(i) the free energy of the hydrogen molecules themselves,

(ii) interactions involving HI, Xe, HBr, or HCl molecules, or

(iii) the external pressure and efficient packing (PV).

In the present cases, the evidence is in favor of packing efficiency: although the HBr, HCl, and HI molecules have dipole moments, the structure persists when they are freely rotating, and the Xe compound is unlikely to be stabilized by long-range Xe-Xe bonds. Furthermore, the hydrogen structure is the same in all compounds at the same lattice parameter, while the intermolecular distances within the supermolecule are highly dependent on density. Explicit treatment of van der Waals interactions is critical at low densities in hydrogen, but of secondary importance at higher pressure [26]. Here van der Waals interactions modeled by the Tkatchenko-Scheffler correction to the PBE functional produced the same structures, further evidence that packing via the PV term in the enthalpy is more important. There is no characteristic supermolecule size. Nevertheless, the pressure is dependent on the minority species.

The hydrogen molecules in the supermolecule show a number of behaviors typical of pure hydrogen at higher pressures. In all cases the H_2 bonds are weaker than those in pure hydrogen at equivalent pressures; this manifests both as longer bond lengths and lower vibrational frequencies. Also, the supermolecule transforms to a broken-symmetry structure at low temperature and rotation becomes inhibited at higher pressures: features observed in pure hydrogen at higher pressures. Hence it is conceivable that upon further pressure increase this supermolecular network might become electrically conducting.

If the molecular-spaced H_{26} cannot be recovered, another possible route to hydrogen storage utilizing $(H_2)_{13}$ is a caged structure with cavities tuned to the size of the supermolecule.

Whether recoverable to ambient conditions or not, these supermolecule compounds have novel and exceptional properties. The combination of extreme stoichiometry and incorporation of fivefold symmetry within a crystal structure is a property previously exhibited by fullerene compounds. The icosahedral supermolecule is stable in a range of environments and will be the basis of a new class of ordered hydrogen-rich compounds.

ACKNOWLEDGMENT

We would like to thank the EPSRC for computing resources through the UKCP project, and we are grateful for support from the ERC "Hecate" fellowship for GJA and from the Royal Society Wolfson Award.

[1] P. Jena, J. Phys. Chem. Lett. **2**, 206 (2011).
[2] N. W. Ashcroft, Phys. Rev. Lett. **92**, 187002 (2004).
[3] A. Drozdov, M. Eremets, I. Troyan, V. Ksenofontov, and S. Shylin, Nature (London) **525**, 73 (2015).
[4] M. Einaga, M. Sakata, T. Ishikawa, K. Shimizu, M. I. Eremets, A. P. Drozdov, I. A. Troyan, N. Hirao, and Y. Ohishi, Nat. Phys. **12**, 835 (2016).
[5] N. W. Ashcroft, Phys. Rev. Lett. **21**, 1748 (1968).
[6] C. J. Pickard and R. J. Needs, Phys. Rev. Lett. **97**, 045504 (2006).
[7] M. Martinez-Canales, A. R. Oganov, Y. Ma, Y. Yan, A. O. Lyakhov, and A. Bergara, Phys. Rev. Lett. **102**, 087005 (2009).
[8] I. Errea, M. Calandra, C. J. Pickard, J. R. Nelson, R. J. Needs, Y. Li, H. Liu, Y. Zhang, Y. Ma, and F. Mauri, Nature (London) **532**, 81 (2016).
[9] S. Zhang, Y. Wang, J. Zhang, H. Liu, X. Zhong, H.-F. Song, G. Yang, L. Zhang, and Y. Ma, Sci. Rep. **5**, 15433 (2015).
[10] G. Zhong, C. Zhang, X. Chen, Y. Li, R. Zhang, and H. Lin, J. Phys. Chem. C **116**, 5225 (2012).
[11] H. Liu, Y. Li, G. Gao, J. S. Tse, and I. I. Naumov, J. Phys. Chem. C **120**, 3458 (2016).
[12] M. Eremets, I. Trojan, S. Medvedev, J. Tse, and Y. Yao, Science **319**, 1506 (2008).
[13] I. Errea, M. Calandra, C. J. Pickard, J. Nelson, R. J. Needs, Y. Li, H. Liu, Y. Zhang, Y. Ma, and F. Mauri, Phys. Rev. Lett. **114**, 157004 (2015).
[14] J. Binns, P. Dalladay-Simpson, M. Wang, G. J. Ackland, E. Gregoryanz, and R. T. Howie, Phys. Rev. B **97**, 024111 (2018).
[15] F. Peng, Y. Sun, C. J. Pickard, R. J. Needs, Q. Wu, and Y. Ma, Phys. Rev. Lett. **119**, 107001 (2017).
[16] C. J. Pickard and R. Needs, J. Phys.: Condens. Matter **23**, 053201 (2011).
[17] Y. Wang, J. Lv, L. Zhu, and Y. Ma, Comput. Phys. Commun. **183**, 2063 (2012).
[18] E. Zurek, R. Hoffmann, N. Ashcroft, A. R. Oganov, and A. O. Lyakhov, Proc. Natl. Acad. Sci. USA **106**, 17640 (2009).
[19] M. Somayazulu, L. Finger, R. Hemley, and H. Mao, Science **271**, 1400 (1996).
[20] J. Binns, X.-D. Liu, P. Dalladay-Simpson, V. Afonina, E. Gregoryanz, and R. T. Howie, Phys. Rev. B **96**, 144105 (2017).
[21] S. J. Clark, M. D. Segall, C. J. Pickard, P. J. Hasnip, M. I. Probert, K. Refson, and M. C. Payne, Z. Kristallogr. **220**, 567 (2005).
[22] C. Lee, W. Yang, and R. G. Parr, Phys. Rev. B **37**, 785 (1988).
[23] A. D. Becke, Phys. Rev. A **38**, 3098 (1988).
[24] R. C. Clay, III, J. Mcminis, J. M. McMahon, C. Pierleoni, D. M. Ceperley, and M. A. Morales, Phys. Rev. B **89**, 184106 (2014).
[25] S. Azadi and W. M. C. Foulkes, Phys. Rev. B **88**, 014115 (2013).
[26] S. Azadi and G. J. Ackland, Phys. Chem. Chem. Phys. **19**, 21829 (2017).
[27] J. P. Perdew, K. Burke, and M. Ernzerhof, Phys. Rev. Lett. **77**, 3865 (1996).
[28] J. P. Perdew, A. Ruzsinszky, G. I. Csonka, O. A. Vydrov, G. E. Scuseria, L. A. Constantin, X. Zhou, and K. Burke, Phys. Rev. Lett. **100**, 136406 (2008).
[29] J. P. Perdew and A. Zunger, Phys. Rev. B **23**, 5048 (1981).
[30] A. Tkatchenko and M. Scheffler, Phys. Rev. Lett. **102**, 073005 (2009).
[31] G. J. Ackland and I. B. Magdău, Cogent Phys. **2**, 1049477 (2015).
[32] S. A. Bonev, E. Schwegler, T. Ogitsu, and G. Galli, Nature (London) **431**, 669 (2004).
[33] H. Liu, L. Zhu, W. Cui, and Y. Ma, J. Chem. Phys. **137**, 074501 (2012).
[34] H. Liu, H. Wang, and Y. Ma, J. Phys. Chem. C **116**, 9221 (2012).

[35] I. B. Magdău and G. J. Ackland, Phys. Rev. B **87**, 174110 (2013).
[36] I. B. Magdău and G. J. Ackland, J. Phys.: Conf. Ser. **500**, 032012 (2014).
[37] R. T. Howie, I. B. Magdău, A. F. Goncharov, G. J. Ackland, and E. Gregoryanz, Phys. Rev. Lett. **113**, 175501 (2014).
[38] I. B. Magdău, M. Marques, B. Borgulya, and G. J. Ackland, Phys. Rev. B **95**, 094107 (2017).
[39] D. P. Shoemaker, R. E. Marsh, F. J. Ewing, and L. Pauling, Acta Crystallogr. **5**, 637 (1952).
[40] K. J. Nordell and G. J. Miller, Inorg. Chem. **38**, 579 (1999).
[41] M. Eldridge, P. Madden, and D. Frenkel, Mol. Phys. **79**, 105 (1993).
[42] A. B. Schofield, P. N. Pusey, and P. Radcliffe, Phys. Rev. E **72**, 031407 (2005).
[43] A. N. Jackson and G. J. Ackland, Phys. Rev. E **76**, 066703 (2007).
[44] See Supplemental Material at http://link.aps.org/supplemental/10.1103/PhysRevMaterials.2.093601 for two mpg movies of the molecular dynamics trajectories. We show a typical halide + supermolecule simulation, with iodane at 300 K and a 10 A supercell: notice the inhibited rotation of the molecules. We also show the Xe + supermolecule at 100 K and 11 A supercell: notice that molecular orientation has stopped and the supermolecule has broken its icosahedral symmetry.
[45] M. Somayazulu, P. Dera, A. F. Goncharov, S. A. Gramsch, P. Liermann, W. Yang, Z. Liu, H.-k. Mao, and R. J. Hemley, Nat. Chem. **2**, 50 (2010).
[46] M. Somayazulu, P. Dera, J. Smith, and R. J. Hemley, J. Chem. Phys. **142**, 104503 (2015).
[47] T. Kaewmaraya, D. Y. Kim, S. Lebegue, C. J. Pickard, R. J. Needs, and R. Ahuja, Phys. Rev. B **84**, 092101 (2011).
[48] U. Pinsook and G. J. Ackland, Phys. Rev. B **59**, 13642 (1999).
[49] G. Ackland and I. Magdău, High Pressure Res. **34**, 198 (2014).
[50] Using the P$ca2_1$ structure, a candidate for the ordered hydrogen phase II.
[51] D. J. Wales and J. P. Doye, J. Phys. Chem. A **101**, 5111 (1997).
[52] J. E. Cuervo and P.-N. Roy, J. Chem. Phys. **125**, 124314 (2006).
[53] J. Martínez, M. Isla, and J. Alonso, Eur. Phys. J. D **43**, 61 (2007).